Seismic waves generated by an impulsive point source in a solid/fluid configuration with a plane boundary

Adrianus T. de Hoop* and Jos H. M. T. van der Hijden‡

GEOPHYSICS, VOL. 50, NO. 7 (JULY 1985); P. 1083–1090, 7 FIGS., 1 TABLE

GEOPHYSICS, VOL. 50, NO. 7 (JULY 1985); P. 1083–1090, 7 FIGS., 1 TABLE

Seismic waves generated by an impulsive point source in a solid/fluid configuration with a plane boundary

Adrianus T. de Hoop* and Jos H. M. T. van der Hijden‡

ABSTRACT

The space-time acoustic wave motion generated by an impulsive point source in a solid/fluid configuration with a vertical plane boundary is calculated with the aid of the modified Cagniard method. Two types of sources are considered in detail, viz. (1) a point source of expansion (model for an explosive source), and (2) a point force parallel to the vertical interface (model for a mechanical vibrator). Numerical results are presented for the transmitted scalar traction in the fluid in those regions of space where head wave contributions occur. There is a marked difference in the time response observed for the two types of sources and for the different positions of the receiver in the fluid with respect to the position of the source in the solid. These waveform differences are important when the transmitted wave in the fluid is used to determine experimentally the elastic properties of the solid. Scholte waves are observed only when the source is close to the fluid/solid interface. As compared with the traditional Fourier-Bessel integral transform method of handling this problem, the computation time with the method presented here is considerably less.

INTRODUCTION

Seismic waves are one standard diagnostic tool used to determine the mechanical parameters (volume density of mass, compressibility, elastic stiffness) and the geometry of subsurface structures. More specifically, in vertical seismic profiling seismic waves are usually generated in the formation (solid), while signals are received in a fluid-filled borehole (Hardage, 1983). Although vertical seismic profiles (VSPs) are usually recorded with clamped geophones, the pressure response of the fluid is also of interest, e.g., when studying the effect on the geophone response or when investigating the possibility of collecting the data with hydrophones. In this kind of measurement transfer of the seismic waves across the boundary of a solid and a fluid always occurs, no matter how simple or how complicated the structure being investigated. Here we investigate the features of this wave transfer in the simplest possible case where there is only a single vertical boundary between a semiinfinite solid and a semiinfinite fluid. As such, the configuration serves as a canonical problem. Results of the calculation clearly show the relative importance of several different parameters on the received signal. Therefore, the results can serve as a guide to the interpretation of experimental data acquired in more complicated situations met in practice.

The seismic source is assumed to be located in the solid, while the acoustic wave is observed in the fluid. The case where the source is located in the fluid (borehole) and the acoustic wave is also observed in the fluid is investigated in a separate paper (de Hoop and van der Hijden, 1984).

The standard approach to the problem is to employ a Fourier transform with respect to time, a Fourier series expansion with respect to the angular variable, and a Fourier-Bessel transform with respect to the radial variable (the latter two in the plane parallel to the boundary). To obtain numerical results, the relevant inverse transforms have to be evaluated numerically, with possible use of asymptotic evaluation in certain regions of space-time. This set-up of the problem is similar to that shown in Aki and Richards (1980, p. 200) for a fluid/fluid configuration. We solve the problem by applying the first author's modification of Cagniard's method (de Hoop, 1960, 1961; see also Miklowitz, 1978, p. 302, and Aki and Richards, 1980, p. 224). The answer has a fairly simple form: the time convolution of the input signal of the source and the explicitly obtained expression, in the form of a bounded integral, for the space-time Green's function of the fluid/solid configuration. The space-time Green's function (or "systems response") clearly shows the features of the time behavior of the elastic/acoustic wave fields at different locations, and the dependence of these wave fields on the mechanical parameters involved. The computational results can also be used as a check on the accuracy of the numerical procedures employed to evaluate the inversion integrals in the standard treatment of the problem. These inversion techniques are the only available procedure that can be used if the materials have an arbitrary loss mechanism, or if the geometries involve curved surfaces such as boreholes.

Manuscript received by the Editor August 13, 1984; revised manuscript received January 11, 1985.
*Schlumberger-Doll Research, P. O. Box 307, Ridgefield, CT 06877; on leave from Delft University of Technology, Department of Electrical Engineering, Laboratory of Electromagnetic Research, P. O. Box 5031, 2600 GA Delft, The Netherlands.
‡Schlumberger-Doll Research, P. O. Box 307, Ridgefield, CT 06877.

DESCRIPTION OF THE CONFIGURATION

We investigate theoretically the pulsed elastic wave motion in a two-media configuration with a vertical plane interface. One of the media is a homogeneous, isotropic, perfectly elastic solid; the other is a homogeneous, ideal fluid. The source is located in the solid. The source generates an impulsive wave motion that is partly reflected at and partly transmitted across the interface. We determine an expression for the acoustic pressure of the transmitted wave at any point in the fluid, and at any time, with the aid of the three-dimensional (3-D) version of the modified Cagniard method.

To specify position in the configuration (Figure 1), we employ Cartesian coordinates ($x_1 = x$, $x_2 = y$, $x_3 = z$) with respect to a Cartesian reference frame with origin O and three mutually perpendicular base vectors of unit length ($\mathbf{i}_1 = \mathbf{i}_x$, $\mathbf{i}_2 = \mathbf{i}_y$, $\mathbf{i}_3 = \mathbf{i}_z$). In the indicated order, the base vectors form a right-handed system. The z-axis is chosen normal to the vertical interface between the two media. (This choice deviates from borehole practice where the z-axis is usually taken along the axis of the borehole, but it is the customary choice for horizontally layered configurations.) The seismic source is located at $x = 0$, $y = 0$, $z = h_T$ with $h_T > 0$. The nature of the source will be specified later. The receiver is located at $x = d$, $y = 0$, $z = -h_R$, with $d > 0$, $h_R > 0$. Additional properties of the configuration are listed in Table 1.

The time coordinate is denoted t. It is assumed that the source starts to act at the instant $t = 0$ and that prior to this instant the entire configuration is at rest.

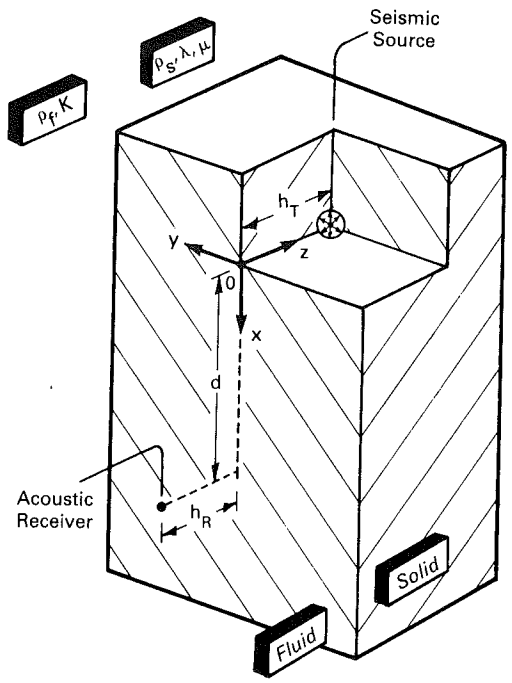

FIG. 1. Solid/fluid configuration with seismic source in solid and acoustic receiver in fluid.

DESCRIPTION OF THE WAVE MOTION IN THE CONFIGURATION

In the solid, the elastic wave motion consists of superposition of incident and reflected waves. The incident wave is the wave that would be generated by the source if the solid were of infinite extent. The incident wave field can be regarded as a proper superposition of P-, SV-, and SH-waves, with the decomposition into these three modes being carried out with respect to the interface so that V means perpendicular to and H means parallel to the interface. The amplitudes of the different wave field constituents are determined by the nature of the source. The incident wave is defined in all space, and in the domain $0 < z < h_T$; its constituents travel in the direction of decreasing z. The reflected wave is defined in the domain $0 < z < \infty$, and it, too, consists of a superposition of P-, SV-, and SH-waves. Its constituents travel in the direction of increasing z. In the fluid, there is a transmitted acoustic wave. It is defined in the domain $-\infty < z < 0$ and travels in the direction of decreasing z. The amplitudes of the reflected P-, SV-, and SH-waves in the solid and of the transmitted wave in the fluid follow from the application of the boundary conditions at the interface.

In the modified Cagniard method we first calculate the wave constituents in the transformed domain, i.e., after having carried out a one-sided Laplace transform with respect to time (with real, positive, transform parameters s) and a Fourier transform with respect to the coordinates x and y parallel to the interface (with transform parameters $s\alpha$ and $s\beta$, respectively). In our notation, we write the relevant transforms for a component of the particle displacement:

$$\hat{u}(x, y, z, s) = \int_0^\infty \exp(-st) u(x, y, z, t)\, dt, \tag{1}$$

$$\tilde{u}(\alpha, \beta, z, s) = \int_{-\infty}^{\infty} dy \int_{-\infty}^{\infty} \exp[is(\alpha x + \beta y)] \times \hat{u}(x, y, z, s)\, dx, \tag{2}$$

and, relative to equation (2), inversely

$$\hat{u}(x, y, z, s) = (s/2\pi)^2 \int_{-\infty}^{\infty} d\beta \int_{-\infty}^{\infty} \exp[-is(\alpha x + \beta y)] \times \tilde{u}(\alpha, \beta, z, s)\, d\alpha. \tag{3}$$

In equation (3) we have taken into account that the transform parameters in equation (2) are $s\alpha$ and $s\beta$.

Each wave consituent is cast in a form that reflects its basic properties. Thus, the P-waves and the wave in the fluid are curl free; the SV- and the SH-waves are divergence free; and the SH-wave has no component of the particle displacement perpendicular to the interface. The easiest way to obtain the expressions is to use the relevant scalar and one-component vector potentials (Stratton, 1941, p. 349).

Incident P-wave

The transform-domain representation of the particle displacement of the incident P-wave is written as

$$\{\tilde{u}_x^{i,P}, \tilde{u}_y^{i,P}, \tilde{u}_z^{i,P}\} = \{-i\alpha, -i\beta, \gamma_P\} A_P^i \exp[s\gamma_P(z - h_T)], \tag{4}$$

where

$$\gamma_P = (\alpha^2 + \beta^2 + s_P^2)^{1/2} \quad \text{with Re } (\gamma_P) \geq 0. \tag{5}$$

Equation (4) takes into account that the incident P-wave is rotation free and that it travels with speed c_P toward the interface. In the calculations we also need the xz, yz, and zz components of the stress τ. They are obtained by substituting the expressions for the particle displacement into the constitutive relations of the solid. For the incident P-wave, they have the form

$$\{\tilde{\tau}_{xz}^{i,P}, \tilde{\tau}_{yz}^{i,P}, \tilde{\tau}_{zz}^{i,P}\} = \{-i\alpha\gamma_P, -i\beta\gamma_P, \tfrac{1}{2}s_S^2 + \alpha^2 + \beta^2\} \times 2\mu s A_P^i \exp[s\gamma_P(z - h_T)]. \tag{6}$$

Incident SV-wave

The transform-domain representation of the particle displacement of the incident SV-wave is written as

$$\{\tilde{u}_x^{i,SV}, \tilde{u}_y^{i,SV}, \tilde{u}_z^{i,SV}\} = \{-i\alpha\gamma_S, -i\beta\gamma_S, \alpha^2 + \beta^2\} A_{SV}^i \exp[s\gamma_S(z - h_T)], \tag{7}$$

where

$$\gamma_S = (\alpha^2 + \beta^2 + s_S^2)^{1/2} \quad \text{with Re } (\gamma_S) \geq 0. \tag{8}$$

Equation (7) takes into account that the incident SV-wave is divergence free and that it travels with speed c_S toward the interface. The xz, yz, and zz components of the stress τ of this wave are

$$\{\tilde{\tau}_{xz}^{i,SV}, \tilde{\tau}_{yz}^{i,SV}, \tilde{\tau}_{zz}^{i,SV}\} = \{-i\alpha(\tfrac{1}{2}s_S^2 + \alpha^2 + \beta^2), -i\beta(\tfrac{1}{2}s_S^2 + \alpha^2 + \beta^2), (\alpha^2 + \beta^2)\gamma_S\} 2\mu s A_{SV}^i \exp[s\gamma_S(z - h_T)]. \tag{9}$$

Incident SH-wave

The transform-domain representation of the particle displacement of the incident SH-wave is written as

$$\{\tilde{u}_x^{i,SH}, \tilde{u}_y^{i,SH}, \tilde{u}_z^{i,SH}\} = \{-i\beta, i\alpha, 0\} A_{SH}^i \exp[s\gamma_S(z - h_T)]. \tag{10}$$

Equation (10) takes into account that the incident SH-wave, too, is divergence free and that it travels with speed c_S toward the interface. The xz, yz, and zz components of the stress of this wave are

$$\{\tilde{\tau}_{xz}^{i,SH}, \tilde{\tau}_{yz}^{i,SH}, \tilde{\tau}_{zz}^{i,SH}\} = \{-i\beta\gamma_S, i\alpha\gamma_S, 0\}\mu s A_{SH}^i \exp[s\gamma_S(z - h_T)]. \tag{11}$$

Reflected P-wave

The transform-domain representation of the particle displacement of the reflected P-wave is written as

$$\{\tilde{u}_x^{r,P}, \tilde{u}_y^{r,P}, \tilde{u}_z^{r,P}\} = \{-i\alpha, -i\beta, -\gamma_P\}[R_{PP} A_P^i \exp(-s\gamma_P h_T) + R_{PS} A_{SV}^i \exp(-s\gamma_S h_T)] \exp(-s\gamma_P z). \tag{12}$$

Equation (12) takes into account that the reflected P-wave is rotation free and that it travels with speed c_P away from the interface. The xz, yz, and zz components of the stress of this wave follow as

$$\{\tilde{\tau}_{xz}^{r,P}, \tilde{\tau}_{yz}^{r,P}, \tilde{\tau}_{zz}^{r,P}\} = \{i\alpha\gamma_P, i\beta\gamma_P, \tfrac{1}{2}s_S^2 + \alpha^2 + \beta^2\} 2\mu s \times [R_{PP} A_P^i \exp(-s\gamma_P h_T) + R_{PS} A_{SV}^i \exp(-s\gamma_S h_T)] \exp(-s\gamma_P z). \tag{13}$$

Reflected SV-wave

The transform-domain representation of the particle displacement of the reflected SV-wave is written as

$$\{\tilde{u}_x^{r,SV}, \tilde{u}_y^{r,SV}, \tilde{u}_z^{r,SV}\} = \{i\alpha\gamma_S, i\beta\gamma_S, \alpha^2 + \beta^2\} \times [R_{SP} A_P^i \exp(-s\gamma_P h_T) + R_{SS} A_{SV}^i \exp(-s\gamma_S h_T)] \exp(-s\gamma_S z). \tag{14}$$

Equation (14) takes into account that the reflected SV-wave is divergence free and that it travels with speed c_S away from the interface. The xz, yz, and zz components of the stress of this wave have the form

$$\{\tilde{\tau}_{xz}^{r,SV}, \tilde{\tau}_{yz}^{r,SV}, \tilde{\tau}_{zz}^{r,SV}\} = \{-i\alpha(\tfrac{1}{2}s_S^2 + \alpha^2 + \beta^2), -i\beta(\tfrac{1}{2}s_S^2 + \alpha^2 + \beta^2), -(\alpha^2 + \beta^2)\gamma_S\} 2\mu s [R_{SP} A_P^i \exp(-s\gamma_P h_T) + R_{SS} A_{SV}^i \exp(-s\gamma_S h_T)] \exp(-s\gamma_S z). \tag{15}$$

Reflected SH-wave

The transform-domain representation of the particle displacement of the reflected SH-wave is obtained as

$$\{\tilde{u}_x^{r,SH}, \tilde{u}_y^{r,SH}, \tilde{u}_z^{r,SH}\} = \{-i\beta, i\alpha, 0\} A_{SH}^i \exp[-s\gamma_S(z + h_T)]. \tag{16}$$

Equation (16) takes into account that the reflected SH-wave, too, is divergence free and that it travels with speed c_S away from the interface. Further, the amplitude is directly obtained by inspection of the boundary conditions at the interface, observing the decoupling of this wave from the P- and SV-waves. The xz, yz, and zz components of the stress of this wave are

$$\{\tilde{\tau}_{xz}^{r,SH}, \tilde{\tau}_{yz}^{r,SH}, \tilde{\tau}_{zz}^{r,SH}\}$$

Table 1. Properties of the solid/fluid configuration.

	Solid	Fluid
Domain	D_s	D_f
z coordinate	$0 < z < \infty$	$-\infty < z < 0$
Volume density of mass	ρ_s	ρ_f
Constitutive parameter(s)	λ, μ (Lamé coefficients)	K (bulk modulus of compression)
Wave speeds	$c_P = [(\lambda + 2\mu)/\rho_s]^{1/2}$	$c_f = (K/\rho_f)^{1/2}$
	$c_S = (\mu/\rho_s)^{1/2}$	
Wave slownesses	$s_P = 1/c_P$; $s_S = 1/c_S$	$s_f = 1/c_f$

$$= \{i\beta\gamma_S, -i\alpha\gamma_S, 0\}\mu s A^i_{SH} \exp[-s\gamma_S(z + h_T)]. \quad (17)$$

Transmitted fluid wave

The transform-domain representation of the particle displacement of the transmitted wave in the fluid is written as

$$\{\tilde{u}^f_x, \tilde{u}^f_y, \tilde{u}^f_z\} = \{-i\alpha, -i\beta, \gamma_f\} \times [T_{fP} A^i_P \exp(-s\gamma_P h_T) + T_{fS} A^i_{SV} \exp(-s\gamma_S h_T)] \exp(s\gamma_f z), \quad (18)$$

where

$$\gamma_f = (\alpha^2 + \beta^2 + s_f^2)^{1/2} \quad \text{with Re}(\gamma_f) \geq 0. \quad (19)$$

The traction in the fluid, i.e., the opposite of the pressure, is obtained as

$$\tilde{\tau}^f = s\rho_f [T_{fP} A^i_P \exp(-s\gamma_P h_T) + T_{fS} A^i_{SV} \exp(-s\gamma_S h_T)] \exp(s\gamma_f z). \quad (20)$$

In the expressions for the reflected waves we have taken into account that P- and SV-waves do not create SH-waves at the solid/fluid interface, and vice versa. In the transmitted wave we have taken into account that the incident SH-wave generates no transmitted wave in the fluid. Next, we determine the as yet unknown reflection and transmission coefficients R_{PP}, R_{PS}, R_{SP}, R_{SS}, T_{fP}, and T_{fS} by applying the boundary conditions that are to be satisfied at the solid/fluid interface.

DETERMINATION OF THE REFLECTION AND TRANSMISSION COEFFICIENTS

The boundary conditions at the solid/fluid interface are (1) continuity of the normal component of the particle displacement, (2) the equality of the normal component of the surface traction in the solid and the (scalar) traction in the fluid, and (3) the vanishing of the tangential components of the surface traction in the solid. In the transform domain, these conditions lead to the equations

$$\lim_{z\downarrow 0} (\tilde{u}^{i,P}_z + \tilde{u}^{i,SV}_z + \tilde{u}^{r,P}_z + \tilde{u}^{r,SV}_z) = \lim_{z\uparrow 0} \tilde{u}^f_z, \quad (21)$$

$$\lim_{z\downarrow 0} (\tilde{\tau}^{i,P}_{zz} + \tilde{\tau}^{i,SV}_{zz} + \tilde{\tau}^{r,P}_{zz} + \tilde{\tau}^{r,SV}_{zz}) = \lim_{z\uparrow 0} \tilde{\tau}^f, \quad (22)$$

$$\lim_{z\downarrow 0} (\tilde{\tau}^{i,P}_{xz} + \tilde{\tau}^{i,SV}_{xz} + \tilde{\tau}^{r,P}_{xz} + \tilde{\tau}^{r,SV}_{xz}) = 0, \quad (23)$$

and

$$\lim_{z\downarrow 0} (\tilde{\tau}^{i,P}_{yz} + \tilde{\tau}^{i,SV}_{yz} + \tilde{\tau}^{r,P}_{yz} + \tilde{\tau}^{r,SV}_{yz}) = 0. \quad (24)$$

Substituting the relevant expressions in these equations, and keeping in mind that the resulting equalities must hold irrespective of the values of A^i_P and A^i_{SV}, we obtain

$$R_{PP} = \{\rho_f\gamma_P s_S^4/4\rho_s - \gamma_f[(\tfrac{1}{2}s_S^2 + \alpha^2 + \beta^2)^2 + (\alpha^2 + \beta^2)\gamma_P\gamma_S]\}/\Delta_{SCH}, \quad (25)$$

$$R_{SP} = -2(\tfrac{1}{2}s_S^2 + \alpha^2 + \beta^2)\gamma_f\gamma_P/\Delta_{SCH}, \quad (26)$$

$$T_{fP} = s_S^2(\tfrac{1}{2}s_S^2 + \alpha^2 + \beta^2)\gamma_P/\Delta_{SCH}, \quad (27)$$

$$R_{PS} = -2(\alpha^2 + \beta^2)(\tfrac{1}{2}s_S^2 + \alpha^2 + \beta^2)\gamma_f\gamma_S/\Delta_{SCH}, \quad (28)$$

$$R_{SS} = -\{\rho_f\gamma_P s_S^4/4\rho_s + \gamma_f[(\tfrac{1}{2}s_S^2 + \alpha^2 + \beta^2)^2 + (\alpha^2 + \beta^2)\gamma_P\gamma_S]\}/\Delta_{SCH}, \quad (29)$$

$$T_{fS} = s_S^2(\alpha^2 + \beta^2)\gamma_P\gamma_S/\Delta_{SCH}, \quad (30)$$

where

$$\Delta_{SCH} = \rho_f\gamma_P s_S^4/4\rho_s + \gamma_f[(\tfrac{1}{2}s_S^2 + \alpha^2 + \beta^2)^2 - (\alpha^2 + \beta^2)\gamma_P\gamma_S] \quad (31)$$

is the "Scholte-wave denominator." The Scholte-wave denominator is associated with surface waves along a solid/fluid interface (Scholte, 1948, 1949; see also Cagniard, 1962, p. 245, and Miklowitz, 1978, p. 168).

The transform-domain expressions for the wave motion in the configuration are now fully determined, once the incident seismic waves are specified. The transformation of these expressions to the space-time domain is carried out in subsequent sections. Explicit results are given for the scalar traction in the fluid for two types of seismic source, viz., (1) a point source of expansion (model for an explosive source), and (2) a point force parallel to the vertical interface (model for a mechanical vibrator).

THE TRANSFORM-DOMAIN INCIDENT WAVE AMPLITUDES

We now determine the transform-domain expressions for the amplitudes A^i_P, A^i_{SV}, and A^i_{SH} of the incident wave. Two types of seismic sources are considered: (1) a point source of expansion (model for an explosive source), and (2) a point force parallel to the vertical interface (model for a mechanical vibrator).

Point source of expansion

The explosive source is modeled by a point source of expansion. The transform-domain expression for the particle displacement is

$$\{\tilde{u}^i_x, \tilde{u}^i_y, \tilde{u}^i_z\} = -\{-i\alpha, -i\beta, \mp\gamma_P\}(\hat{\phi}_V/2s\gamma_P) \times \exp[\mp s\gamma_P(z - h_T)], \quad (32)$$

where the upper signs apply to $z > h_T$ and the lower signs to $z < h_T$, and $\phi_V = \phi_V(t)$ is the time rate of injected volume at the source. By comparing equation (32) with equations (4), (7), and (10), we obtain

$$A^i_P = -\hat{\phi}_V/2s\gamma_P, \quad (33)$$

$$A^i_{SV} = 0, \quad (34)$$

and

$$A^i_{SH} = 0. \quad (35)$$

This type of source generates a P-wave, and no SV- or SH-waves.

Point force parallel to the interface

The action of a mechanical vibrator is modeled by a point force acting in the x direction (vertical force in the presence of a vertical boundary in borehole seismics). The transform-domain expressions for the components of the particle displacement are (Achenbach, 1973, p. 99; Aki and Richards, 1980, p. 73; Miklowitz, 1978, p. 89)

$$\hat{u}_x^i = (\hat{F}_V/2s\rho_s)\{-\alpha^2\gamma_P^{-1}\exp[\mp s\gamma_P(z-h_T)] + (\alpha^2+s_S^2)\gamma_S^{-1}\exp[\mp s\gamma_S(z-h_T)]\}, \quad (36)$$

$$\hat{u}_y^i = (\hat{F}_V/2s\rho_s)\{-\alpha\beta\gamma_P^{-1}\exp[\mp s\gamma_P(z-h_T)] + \alpha\beta\gamma_S^{-1}\exp[\mp s\gamma_S(z-h_T)]\}, \quad (37)$$

and

$$\hat{u}_z^i = (\hat{F}_V/2s\rho_s)\{\pm i\alpha\exp[\mp s\gamma_P(z-h_T)] \pm i\alpha\exp[\mp s\gamma_S(z-h_T)]\}, \quad (38)$$

where the upper signs apply to $z > h_T$ and the lower signs to $z < h_T$, and $F_V = F_V(t)$ is the applied force. By comparing equations (36) through (38) with equations (4), (7), and (10), we obtain

$$A_P^i = -i\alpha\hat{F}_V/2s\rho_s\gamma_P, \quad (39)$$

$$A_{SV}^i = i\alpha\hat{F}_V/2s\rho_s(\alpha^2+\beta^2), \quad (40)$$

and

$$A_{SH}^i = i\beta\hat{F}_V/2s\rho_s c_S^2\gamma_S(\alpha^2+\beta^2). \quad (41)$$

This type of source generates P- and SV-waves as well as SH-waves.

SPACE-TIME EXPRESSION FOR THE SCALAR TRACTION IN THE FLUID DUE TO A POINT SOURCE OF EXPANSION IN THE SOLID

To arrive at the space-time expression for the scalar traction in the fluid τ^f (i.e., the opposite of the pressure) due to a point source of expansion in the solid, we rewrite equation (20) at the position of the receiver $x = d$, $y = 0$, $z = -h_R$ as

$$\tilde{\tau}^f = s^2\hat{\phi}_V\tilde{\tau}_P^{f,G}, \quad (42)$$

where, as a result of equation (27) and equations (33) through (35), we have

$$\tilde{\tau}_P^{f,G} = -\frac{\rho_f(\frac{1}{2}s_S^2+\alpha^2+\beta^2)}{2s^2c_S^2\Delta_{SCH}} \times \exp[-s(\gamma_P h_T + \gamma_f h_R)]. \quad (43)$$

Starting from equation (43), the expression for $\tau_P^{f,G}$ is obtained with the aid of the modified Cagniard method. This method accomplishes the transformation of the integration with respect to α and β [cf., equation (3)]

$$\hat{\tau}_P^{f,G} = -(s/2\pi)^2\int_{-\infty}^{\infty}d\beta\int_{-\infty}^{\infty}\frac{\rho_f(\frac{1}{2}s_S^2+\alpha^2+\beta^2)}{2s^2c_S^2\Delta_{SCH}} \times \exp\{-s[i\alpha x + i\beta\gamma + \gamma_P h_T + \gamma_f h_R]\}\,d\alpha \quad (44)$$

into the real integration

$$\hat{\tau}_P^{f,G}(\cdot,s) = \int_T^{\infty}\exp(-s\tau)\Gamma(\cdot,\tau)\,d\tau, \quad (45)$$

where $\Gamma(\cdot,\tau)$ is an expression that does not depend upon s and where the dot stands for the spatial variables. The uniqueness theorem of the Laplace transform with real, positive transform parameter s then ensures that (Lerch's theorem, see Widder, 1946, p. 63),

$$\tau_P^{f,G}(\cdot,\tau) = \begin{cases}0 & \text{when } -\infty < \tau < T,\\ \Gamma(\cdot,\tau) & \text{when } T < \tau < \infty.\end{cases} \quad (46)$$

Here, T is the arrival time of the transmitted wave. The actual transformations follow the pattern of the modified Cagniard method for 3-D wave motion (see Appendix A). Equation (42) then leads to the final result

$$\tau^f(\cdot,t) = \partial_t^2\int_0^t\phi_V(t-\tau)\,\tau_P^{f,G}(\cdot,\tau)\,d\tau \quad (47)$$

when $0 < t < \infty$.

SPACE-TIME EXPRESSION FOR THE SCALAR TRACTION IN THE FLUID DUE TO A POINT FORCE PARALLEL TO THE INTERFACE IN THE SOLID

To arrive at the space-time expression for the scalar traction in the fluid due to a point force parallel to the interface in the solid, we rewrite equation (20) at the position of the receiver $x = d$, $y = 0$, $z = -h_R$ as

$$\tilde{\tau}^f = s^2\hat{F}_V(\tilde{\tau}_P^{f,G} + \tilde{\tau}_{SV}^{f,G}), \quad (48)$$

where because of equations (27) and (30) and equations (39) through (41) we have

$$\tilde{\tau}_P^{f,G} = -\frac{i\alpha(\frac{1}{2}s_S^2+\alpha^2+\beta^2)\rho_f}{2s^2\rho_s c_S^2\Delta_{SCH}} \times \exp[-s(\gamma_P h_T + \gamma_f h_R)], \quad (49)$$

and

$$\tilde{\tau}_{SV}^{f,G} = \frac{i\alpha\gamma_P\gamma_S\rho_f}{2s^2\rho_s c_S^2\Delta_{SCH}}\exp[-s(\gamma_S h_T + \gamma_f h_R)]. \quad (50)$$

Using arguments of the same type as in the previous section, the space-time expression for the scalar traction in the fluid is obtained as

$$\tau^f(\cdot,t) = \partial_t^2\int_0^t F_V(t-\tau)[\tau_P^{f,G}(\cdot,\tau) + \tau_{SV}^{f,G}(\cdot,\tau)]\,d\tau, \quad (51)$$

when $0 < t < \infty$, where the dot stands for the spatial variables, and $\tau_P^{f,G}$ and $\tau_{SV}^{f,G}$ are constructed with the aid of the modified Cagniard method.

NUMERICAL RESULTS

We now present some curves showing τ^f as a function of t, computed according to equations (47) and (51) with the appropriate expressions for the Green's function contributions. These curves represent, for the model configuration at hand, the synthetic seismograms that apply to VSP configurations. For details of the numerical methods employed, we refer to de Hoop and van der Hijden (1984) [in that paper an erroneous factor of 2 is present in equation (B-3); as a consequence the vertical scales in the figures representing the numerical results have to be divided by 2]. In particular, we want to illustrate how the offset of the source from the boundary influences the received pressure waveforms in the fluid. To this end, synthetic waveforms are shown that are recorded by a receiver at a depth of 1 600 m, or by an array of receivers at depths extending from 1 000 m to 1 600 m. The seismic source will be located at offsets of 10, 400, or 1 000 m from the boundary. The results show that sources at different offsets from the boundary can give rise to very different types of recorded waveforms in the fluid. In borehole seismics, the question of

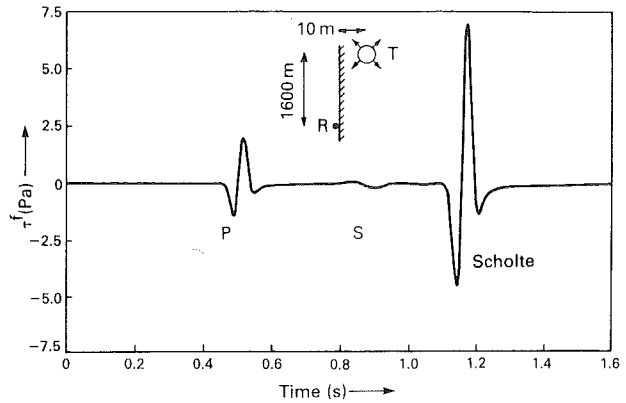

FIG. 2. Scalar traction τ^f in the fluid due to an impulsive point source of expansion in the solid as a function of time. The source pulse has a maximum value max $|\phi_V| = (T/2\pi)^2$, and its duration is $T = 0.1$ s. Further, $c_P = 3\ 500$ m/s, $c_S = 2\ 000$ m/s, $c_f = 1\ 500$ m/s, $\rho_s/\rho_f = 2.5$, $d = 1\ 600$ m, $h_T = 10$ m, and $h_R = 0$.

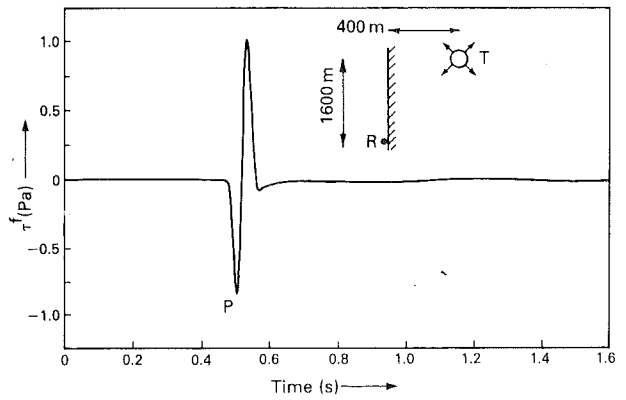

FIG. 3. Scalar traction τ^f in the fluid due to an impulsive point source of expansion in the solid as a function of time. The source pulse has a maximum value max $|\phi_V| = (T/2\pi)^2$, and its duration is $T = 0.1$ s. Further, $c_P = 3\ 500$ m/s, $c_S = 2\ 000$ m/s, $c_f = 1\ 500$ m/s, $\rho_s/\rho_f = 2.5$, $d = 1\ 600$ m, $h_T = 400$ m, and $h_R = 0$.

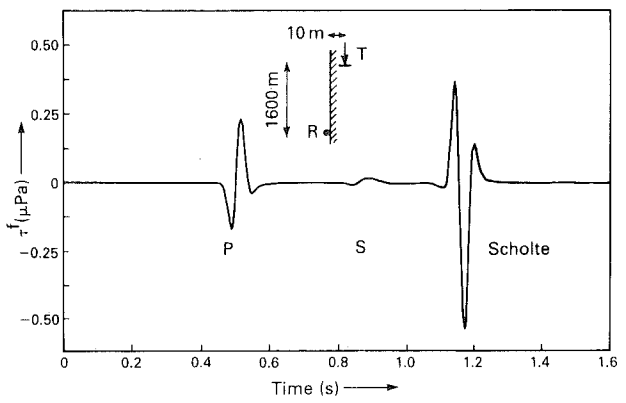

FIG. 4. Scalar traction τ^f in the fluid due to an impulsive point force parallel to the interface in the solid as a function of time. The source pulse has a maximum value max $|F_V| = (T/2\pi)^2$, and its duration is $T = 0.1$ s. Further, $c_P = 3\ 500$ m/s, $c_S = 2\ 000$ m/s, $c_f = 1\ 500$ m/s, $\rho_s/\rho_f = 2.5$, $d = 1\ 600$ m, $h_T = 10$ m, and $h_R = 0$.

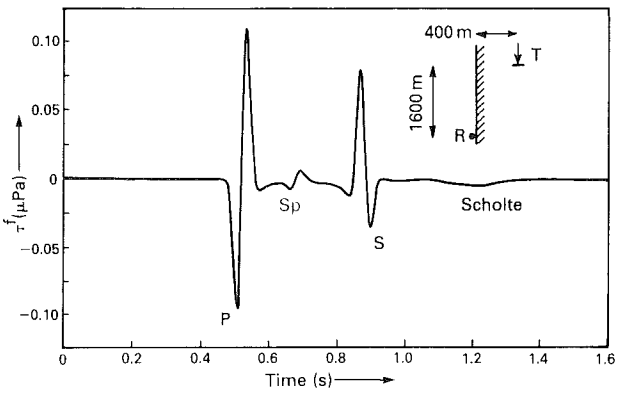

FIG. 5. Scalar traction τ^f in the fluid due to an impulsive point force parallel to the interface in the solid as a function of time. The source pulse has a maximum value max $|F_V| = (T/2\pi)^2$, and its duration is $T = 0.1$ s. Further, $c_P = 3\ 500$ m/s, $c_S = 2\ 000$ m/s, $c_f = 1\ 500$ m/s, $\rho_s/\rho_f = 2.5$, $d = 1\ 600$ m, $h_T = 400$ m, and $h_R = 0$.

how strongly the Stoneley wave (or tube wave) in the borehole is excited is of special interest. In our planar model, this question translates into investigating how strongly the Scholte wave is excited.

Strictly speaking, it is difficult to extrapolate the conclusions pertaining to the planar interface considered here to the ones for a circularly cylindrical interface as in borehole configurations. It can be expected that the phenomena in the two configurations show similar characteristics in the case where the spatial pulse widths of the signals are small compared to the radius of curvature of the interface.

In our model we used the following parameters: $c_P = 3\ 500$ m/s, $c_S = 2\ 000$ m/s, $c_f = 1\ 500$ m/s, $\rho_s/\rho_f = 2.5$. We put the acoustic receiver in the fluid infinitely close to the solid/fluid interface, i.e., at $h_R = 0$. For the time variation of the source strengths $\phi_V(t)$ and $F_V(t)$ (as introduced in the transform-domain incident wave amplitudes discussion), we used the four-point optimum Blackman window function (Harris, 1978) with maximum amplitude equal to $(T/2\pi)^2$, where T is the source pulse duration. Accordingly, we have to convolve the Green's functions occurring in equations (47) and (51) with the second derivative of this function, i.e., with

$$\partial_t^2 \phi_V(t) = \partial_t^2 F_V(t) = \begin{cases} 0 & \text{when } -\infty < t < 0, \\ \sum_{n=0}^{3} (-b_n n^2) \cos(2\pi n t/T) & \\ & \text{when } 0 < t < T, \\ 0 & \text{when } T < t < \infty, \end{cases} \tag{52}$$

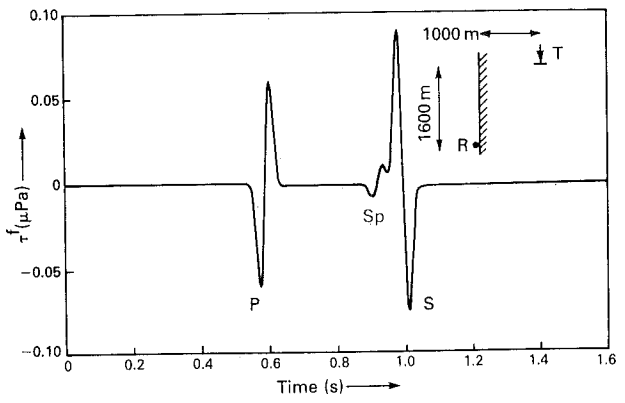

FIG. 6. Scalar traction τ^f in the fluid due to an impulsive point force parallel to the interface in the solid as a function of time. The source pulse has a maximum value max $|F_V| = (T/2\pi)^2$, and its duration is $T = 0.1$ s. Further, $c_P = 3\ 500$ m/s, $c_S = 2\ 000$ m/s, $c_f = 1\ 500$ m/s, $\rho_s/\rho_f = 2.5$, $d = 1\ 600$ m, $h_T = 1\ 000$ m, and $h_R = 0$.

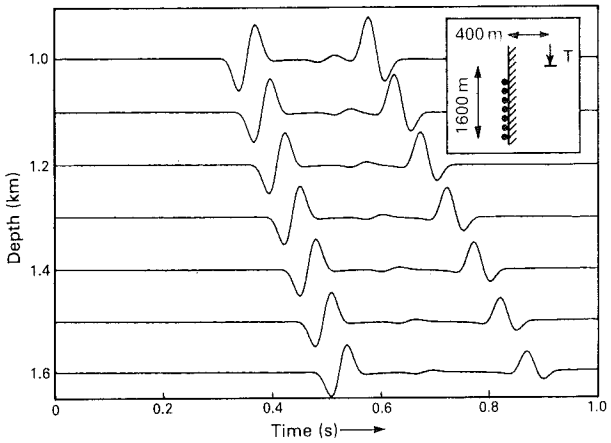

FIG. 7. Scalar traction τ^f at an array of receivers in the fluid due to an impulsive point force parallel to the interface in the solid as a function of time. The receivers are positioned at depths between 1 000 and 1 600 m, at intervals of 100 m. The source pulse has a maximum value max $|F_V| = (T/2\pi)^2$, and its duration is $T = 0.1$ s. Further, $c_P = 3\ 500$ m/s, $c_S = 2\ 000$ m/s, $c_f = 1\ 500$ m/s, $\rho_s/\rho_f = 2.5$, $h_T = 400$ m, and $h_R = 0$.

in which the constants b_n are given by $b_0 = +0.35869$, $b_1 = -0.48829$, $b_2 = +0.14128$, and $b_3 = -0.01168$. This pulse shows great similarity with the classic Ricker wavelet. The source pulse duration is taken to be $T = 0.1$ s; therefore its center frequency is 15.5 Hz.

In Figures 2 and 3, the scalar traction τ^f in the fluid due to an impulsive point source of expansion in the solid is plotted as a function of time. In Figure 2, the offset of the source from the interface is $h_T = 10$ m, while in Figure 3, $h_T = 400$ m. In both figures we clearly see a *P*-wave arrival, but only in Figure 2, where the source is much closer to the solid/fluid interface, do we see a strong Scholte wave arrival. Although a point source of expansion generates only *P*-waves, *S*-waves are created due to mode conversion at the interface. Figure 2 shows this small *S*-wave arrival, but the converted *S*-mode is indistinguishable in Figure 3. The absence of an *S*-wave is understandable in Figure 3 since the ray trajectories are much more toward normal incidence, and hence less *P*-to-*S* conversion takes place.

Figures 4, 5, and 6 show the scalar traction due to an impulsive point force parallel to the interface as a function of time, at offsets $h_T = 10$, 400, and 1 000 m, respectively. In all three figures, the *P*- and *S*-wave arrivals are now clearly visible, while in Figures 5 and 6 the shear head wave arrival *Sp* can also be observed. Again, we see that a Scholte wave arrival is present only if the source is close to the interface. In comparing Figures 2 and 4 we see that the change from an expansion source to a point force does not change the polarity of the *P*-wave, while the polarities of the *S*- and Scholte wave arrivals are reversed. In Figure 6, no Scholte wave is visible because the source is located far from the interface.

Finally, Figure 7 shows synthetic seismograms for an array of receivers at depths between 1 000 and 1 600 m, with a point force at an offset of 400 m. The changing position of the shear head wave in the waveforms relative to the *P*-wave is clearly visible. Further, we see that the amplitude of the *S*-wave decreases strongly with increasing depth due to the radiation pattern of the point force; while for the *P*-wave the radiation pattern of the point force (partly) compensates the decrease with increasing depth.

The time required to compute a synthetic seismogram for the previous figures on a VAX 11/780 computer is about 10 s. This is considerably less time than is needed for the numerical evaluation of the integrals occurring in the standard Fourier-Bessel transform method (Aki and Richards, 1980, p. 200) with which the second author has experience.

CONCLUSION

With the aid of the modified Cagniard method, an expression has been derived for the scalar traction in a semiinfinite fluid when an impulsive point source is present in a semiinfinite solid near a plane interface between the fluid and the solid media. Numerical results illustrate the different waveform features that result when the type of source and the offset of the source in the solid are varied. Numerical evaluation of the expressions requires much less computation time than would be necessary if the analysis were done by evaluating the standard Fourier and Fourier-Bessel inversion integrals.

REFERENCES

Achenbach, J. D., 1973, Wave propagation in elastic solids: North-Holland Publ. Co.

Aki, K., and Richards, P. G., 1980, Quantitative seismology: W. H. Freeman and Co.

Cagniard, L., 1962, Reflection and refraction of progressive seismic waves: McGraw-Hill. [Trans. and rev. of Cagniard, L., 1939, Réflexion et Réfraction des Ondes Séismiques Progressives, Gauthier-Villars, by E. A. Flinn and C. H. Dix.]

Hardage, B. A., 1983, Vertical seismic profiling: Geophysical Press.

Harris, F. J., 1978, On the use of windows for harmonic analysis with the discrete Fourier transform: Proc. Inst. Elect. and Electron. Eng., **66**, 51–83.
de Hoop, A. T., 1960, A modification of Cagniard's method for solving seismic pulse problems: Appl. Sci. Res., Sec. B, **8**, 349–356.
——— 1961, Theoretical determination of the surface motion of a uniform elastic half-space produced by a dilatational, impulsive point source: Proc. Colloque International C.N.R.S. no. 111, Marseille, 21–32 (in English).
de Hoop, A. T., and van der Hijden, J. H. M. T., 1984, Generation of acoustic waves by an impulsive point source in a fluid/solid configuration with a plane boundary: J. Acoust. Soc. Am., **75**, 1709–1715.
Miklowitz, J., 1978, The theory of elastic waves and waveguides: North-Holland Publ. Co.
Scholte, J. G., 1948, On the large displacements commonly regarded as caused by Love waves and similar dispersive surface waves: Proc. K. Ned. Akad. Wet., **51**, 533–543, 642–649, 828–835, 969–976 (in English).
——— 1949, On true and pseudo-Rayleigh waves: Proc. K. Ned. Akad. Wet., **52**, 652–653 (in English).
Stratton, J. A., 1941, Electromagnetic theory: McGraw-Hill Book Co.
Widder, D. V., 1946, The Laplace transform: Princeton Univ. Press.

APPENDIX A
TRANSFORMATIONS IN THE MODIFIED CAGNIARD METHOD

The main steps that lead from equation (44) to equation (45) are briefly indicated here. First, the variables of integration α and β in equation (44) are changed into

$$\alpha = \kappa \cos(\theta) - q \sin(\theta), \tag{A-1}$$

and

$$\beta = \kappa \sin(\theta) + q \cos(\theta), \tag{A-2}$$

where θ follows from the polar-coordinate specification of the point of observation, i.e.,

$$x = r \cos(\theta), \qquad y = r \sin(\theta). \tag{A3}$$

In the integration with respect to κ and q that results, q is kept real, while the integrand is continued analytically into the complex p plane, where $p = i\kappa$. For fixed q, the integration in the complex p plane is carried out along the path where

$$pr + (q^2 - p^2 + s_P^2)^{1/2} h_T + (q^2 - p^2 + s_S^2)^{1/2} h_R = \tau, \tag{A-4}$$

with τ real and positive. Finally, the integrations with respect to τ and q are interchanged, and the resulting integrals with respect to q are (with the aid of the transformation given in Appendix B) transformed into integrals over the fixed range $(0, \pi/2)$. The latter transformation also removes the inverse square-root singularities that can occur at the end points of the q integration. After this, the integrand is smooth, and a simple numerical integration formula suffices to yield results of any desired accuracy.

APPENDIX B
TRANSFORMATION OF THE GREEN'S FUNCTION INTEGRALS FOR NUMERICAL PURPOSES

All integrals that result after applying the transformations of Appendix A are of the type

$$I = \int_{Q_1}^{Q_2} f(q)\, dq, \tag{B-1}$$

with $Q_2 > Q_1$, where $f(q)$ can have inverse square-root singularities at either $q = Q_1$ or $q = Q_2$, or both. Instead of q we introduce the variable of integration ψ through

$$q^2 = Q_1^2 \cos^2(\psi) + Q_2^2 \sin^2(\psi). \tag{B-2}$$

Then the interval $Q_1 < q < Q_2$, where Q_1 and/or Q_2 depend upon the position of observation and on time, is mapped onto the fixed interval $0 < \psi < \pi/2$, while

$$dq = \frac{(Q_2^2 - Q_1^2) \sin(\psi) \cos(\psi)}{[Q_1^2 \cos^2(\psi) + Q_2^2 \sin^2(\psi)]^{1/2}}\, d\psi. \tag{B-3}$$